

# Synthesis and characterization of a novel organophosphorus oligomer and its application in improving flame retardancy of epoxy resin

 Cite this: *RSC Adv.*, 2014, 4, 17607

 Nana Tian,<sup>a</sup> Jiang Gong,<sup>ab</sup> Xin Wen,<sup>a</sup> Kun Yao<sup>ab</sup> and Tao Tang<sup>\*a</sup>

A novel organophosphorus, poly(4,4-dihydroxy-1-methyl-ethyl diphenol-*o*-bicyclic pentaerythritol phosphatephosphate) (PCPBO), was synthesized and characterized by FTIR, <sup>1</sup>H NMR and <sup>31</sup>P NMR. The flame retardancy and thermal stability of epoxy resin with different PCPBO loadings were investigated using the limited oxygen index (LOI), vertical burning test, cone calorimeter test and thermogravimetric analysis. The results showed that the incorporation of PCPBO into epoxy resin (EP) significantly improved its flame retardancy and thermal stability. The reduction of the peak heat release rate, total heat release and the increased char yield at high temperature further confirmed the improvement of the flame retardancy. FT-IR at different temperatures and the scanning electron microscopy of residual char revealed that the addition of PCPBO could induce the formation of an intumescent char layer, which retarded the degradation and combustion process of EP.

 Received 21st February 2014  
 Accepted 3rd April 2014

DOI: 10.1039/c4ra01525h

[www.rsc.org/advances](http://www.rsc.org/advances)

## 1. Introduction

Epoxy resin (EP), with its excellent mechanical strength and insulation characteristics, has been widely used as a high performance resin in many fields such as adhesives, laminates, coatings and electrical insulation.<sup>1–3</sup> However, the flammability is a major drawback of epoxy resin and restricts its applications. Therefore, improving flame retardancy of EP is very important and necessary.<sup>4,5</sup>

In the past decades, halogen-containing compounds are widely used as additive to improve the flame retardancy of epoxy resin. Nevertheless, the main problem is the generation of a large amount of toxic and corrosive gases from these halogen-containing flame retardants during combustion, which leads to environmental pollution.<sup>6,7</sup> Consequently, many researchers pay more attention to exploit the halogen-free flame retardants for epoxy resin. Among the halogen-free systems, epoxy resin modified by phosphorus-containing compounds is considered as efficient method due to its notable flame retardant efficiency.<sup>8–10</sup>

In the recent years, 2,6,7-trioxa-1-phosphabicyclo[2,2,2]-octane-4-methanol (PEPA) and its derivatives, as a novel kind of phosphorous-containing flame retardants, have attracted more attention because of their high reactivity and good charring.<sup>11–14</sup> However, these compounds reported are mostly low molecular weight, which exist many shortcomings such as migration,

leaching and poor compatibility with polymer matrix. Therefore, oligomeric and polymeric flame retardants with more aromatic structure have been proposed to deal with this problem. The polymeric flame retardant modified by PEPA is seldom reported up to now.

In order to improve the flame retardancy of epoxy resins, we synthesized a novel organophosphorus oligomer which contained aryl and caged bicyclic phosphate functional groups at the same time. The chemical structure of this compound was characterized by Fourier transform infrared (FT-IR) and nuclear magnetic resonance (NMR). The thermal degradation behaviors and the flame retardancy were investigated by thermogravimetric analysis (TGA) and cone calorimeter test, respectively.

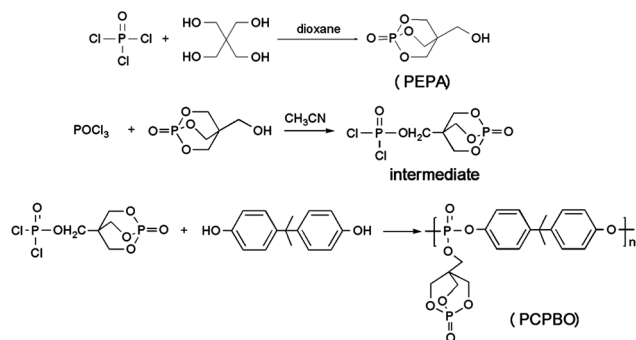
## 2. Experiment part

### 2.1 Materials

The epoxy resin was a DGEBA (diglycidyl ether of bisphenol A) with the epoxide value of 0.48–0.54 provided by Wuxi Lanxing Co., Ltd. Phosphorus oxychloride (POCl<sub>3</sub>), which was distilled under atmospheric pressure before usage, and triethylene tetramine (TETA) were purchased from Guangfu Chemical Research Institute (Tianjin, China). Pentaerythritol (PER) was provided by Fuyu Fine Chemical Co., Ltd (Tianjin, China). Triethylamine (Et<sub>3</sub>N), acetonitrile and dioxane supplied by Fuchen Chemical Reagents Factory (Tianjin, China) were dried with 4 Å molecular sieve and distilled prior to use. Bisphenol A and acetonitrile were provided by Guangfu Fine Chemical Institute (Tianjin, China). 2,6,7-Trioxa-1-phosphabicyclo-[2,2,2]octane-4-methanol (PEPA) was synthesized according to the ref. 15 and recrystallized in alcohol. The synthesis route of PEPA is shown

<sup>a</sup>State Key Laboratory of Polymer Physics and Chemistry, Changchun Institute of Applied Chemistry, Chinese Academy of Sciences, Changchun 130022, China. E-mail: ttang@ciac.ac.cn; Fax: +86 (0)431 85262827; Tel: +86 (0)431 85262004

<sup>b</sup>University of Chinese Academy of Sciences, Beijing 100049, China



Scheme 1 Synthetic route of PCPBO.

in Scheme 1 and its chemical structure was determined by FTIR and  $^1\text{H}$  NMR.

## 2.2 Synthesis of PCPBO

To a three-neck 500 mL glass flask with a thermometer, a reflux and a nitrogen inlet were charged 36 g (0.2 mol) of PEPA, 31 g (0.2 mol) of  $\text{POCl}_3$  and 250 mL of acetonitrile. The reaction mixture was maintained  $80\text{ }^\circ\text{C}$  for 12 h and then cooled to room temperature. After filtration and rotary evaporation, the intermediate was obtained. Then a mixture of 45.5 g (0.2 mol) of bisphenol A and the intermediate dissolved in 250 mL acetonitrile was added into a three-neck 500 mL round bottom flask equipped with a reflux condenser and a constant pressure funnel. 0.2 mol  $\text{Et}_3\text{N}$  was slowly dropwise added to the mixture over a period of 0.5 h at the room temperature and heated to reflux. Thereafter, the reaction was kept at 12 h at the same temperature. Through filtration triethylamine hydrochloride was moved and washed with trichloromethane. The filtrate was combined together and put to rotary evaporator to further purify under reduced pressure. The final product was obtained as light yellow liquid with a yield of 90%. The synthetic route is described in Scheme 1.

## 2.3 Preparation of EP/PCPBO hybrids

The phosphorus-containing epoxy resins were prepared by mixing EP with PCPBO for 10 min under the mechanical stirring. Thereafter the above mixture was mixed homogeneously with TETA in an epoxide/amino equivalent ratio of 1/1. The mixture was poured into a polytetrafluoroethylene mold and cured at room temperature for 2 days, and post cured at  $90\text{ }^\circ\text{C}$

for 2 h. After curing, all samples were cooled to room temperature. The compositions of samples are shown in Table 1.

Samples were thermally treated at a heating rate of  $10\text{ }^\circ\text{C min}^{-1}$  in a muffle furnace in air. The solid residues were obtained when heated to the designed temperature, and maintained at each temperature for 10 min. Then the residues were mixed with KBr powder and pressed into discs for FT-IR analysis.

## 2.4 Characterization and measurement

The FT-IR spectrum was recorded on a Vertex 70 FTIR spectrometer (Bruker, Germany) with KBr pellets. Spectra in the optical range  $400\text{--}4000\text{ cm}^{-1}$  were obtained by averaging 16 scans at a resolution of  $4\text{ cm}^{-1}$ . NMR spectra were registered with a Bruker AV400 NMR spectrometer (400 MHz) using TMS and 85%  $\text{H}_3\text{PO}_4$  as references, respectively, and using  $d_6$ -DMSO as solvent.

The limiting oxygen index (LOI) values were measured on an HC-2C oxygen index meter (Jingning Analysis Instrument Company, China) with sheet dimensions of  $130\text{ mm} \times 6.5\text{ mm} \times 3\text{ mm}$  according to the ASTM D2863-97 standard. The vertical burning tests were tested according to the UL-94 test standard (ASTM D3801, 2010) with the test specimen was  $130 \times 13 \times 3\text{ mm}^3$ .

Differential scanning calorimeter (DSC) was carried out under a nitrogen atmosphere by means of METTLER TOLEDO-DSC1 analyzer from  $25\text{ to }200\text{ }^\circ\text{C}$  at a heating rate of  $10\text{ }^\circ\text{C min}^{-1}$ . The nitrogen flowrate was  $100\text{ mL min}^{-1}$ .

Thermogravimetric analysis (TGA) was carried out with a Q600 thermal analyzer (TA Co., New Castle, USA) from ambient temperature to  $800\text{ }^\circ\text{C}$  at a heating rate of  $10\text{ }^\circ\text{C min}^{-1}$  under both air and nitrogen atmosphere with a flowing rate of  $100\text{ mL min}^{-1}$ . The char morphology was observed by means of field emission scanning electron microscopy (FE-SEM, XL303SEM).

Cone calorimeter tests were performed using an FTT, UK device according to ISO 5660 at an incident flux of  $50\text{ kW m}^{-2}$ , and the size of specimens was  $100\text{ mm} \times 100\text{ mm} \times 6.0\text{ mm}$ ; all samples were burned in triplicate and the data were the average of three replicated tests.

The morphology of the residual chars obtained was examined by means of field emission scanning electron microscopy (XL303SEM). The surface of residual chars was sputter-coated with gold layer before examination.

X-ray photoelectron spectroscopy (XPS) spectra of the char residue was recorded with a VG ESCALAB MK II spectrometer using an Al  $K\alpha$  exciting radiation from an X-ray source operated at  $10.0\text{ kV}$  and  $10\text{ mA}$ .

Table 1 Formulation and flame retardancy of epoxy resin systems

Sample	PCPBO content (wt%)	Flame retardancy	
		LOI	UL-94
EP	0	22.5	Fail
EP1	5	27.3	Fail
EP2	10	28.8	Fail
EP3	15	30.3	V-1
EP4	20	31.2	V-0

## 3. Results and discussion

### 3.1 Characterization of PCPBO

Scheme 1 presents the synthetic route of PCPBO. The chemical structure of PCPBO was characterized with FTIR,  $^1\text{H}$  NMR and  $^{31}\text{P}$  NMR spectra. Fig. 1 shows FTIR spectra of the synthesized PCPBO. The absorption band at about  $3328\text{ cm}^{-1}$  corresponds to the vibration of O-H stretching band, and the peak at  $2969$

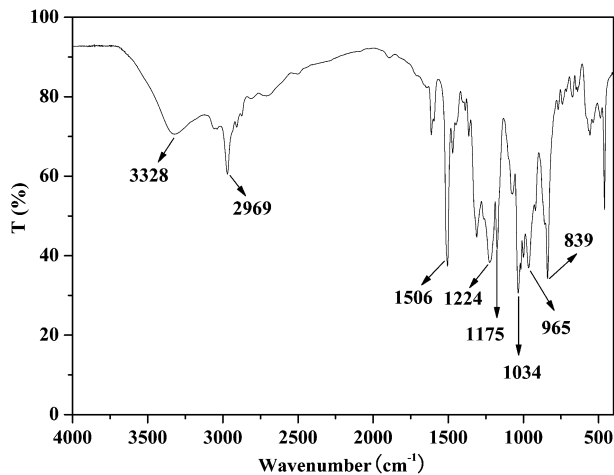


Fig. 1 FT-IR spectrum of PCPBO.

$\text{cm}^{-1}$  is assigned to the vibration of saturated  $\text{CH}_2$  stretching band. The sharp bond at  $1506 \text{ cm}^{-1}$  is associated with  $\text{C}=\text{C}$  in benzene ring. The absorption bands for  $\text{P}=\text{O}$  and  $\text{P}-\text{O}-\text{C}$  stretching vibration appear at  $1224 \text{ cm}^{-1}$  and  $1034 \text{ cm}^{-1}$ , respectively. The absorption at  $839 \text{ cm}^{-1}$  is attributed to the skeleton vibration of caged phosphates.

Fig. 2 illustrates the  $^1\text{H}$  NMR spectra of PCPBO with the assignments of all the protons. The multiplet between 6.64 and 7.25 ppm (c and d) is assigned to the protons of benzene ring. The doublets at 4.60 (a) and 4.15 ppm (b) correspond to  $\text{CH}_2$  protons from the caged bicyclic phosphate and adjacent to the caged ring, respectively. The  $\text{CH}_3$  protons in PCPBO appear from 1.52 and 1.63 ppm (e). The structure of PCPBO was also confirmed by  $^{31}\text{P}$  NMR (Fig. 3). Two sharp signals are observed because of the molecular structure containing two different chemical shifts of phosphorus atoms. The peak of phosphorus (a) adjacent to bisphenol A appears at  $-7.71 \text{ ppm}$ . The peak at  $-11.77 \text{ ppm}$  corresponds to the phosphorus (b) of the caged bicyclic phosphates. From the above analysis, it is confirmed that the target product has been synthesized successfully.

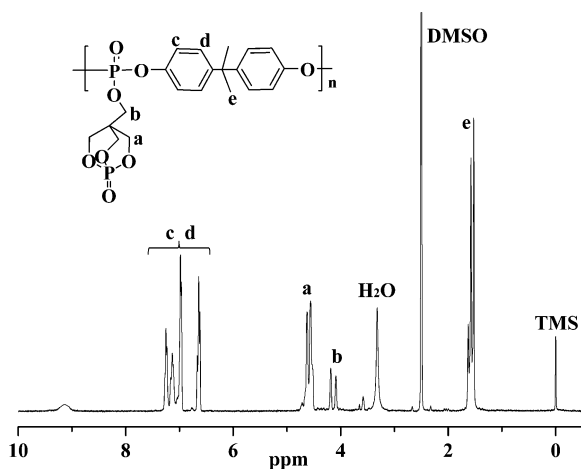


Fig. 2  $^1\text{H}$  NMR spectrum of PCPBO.

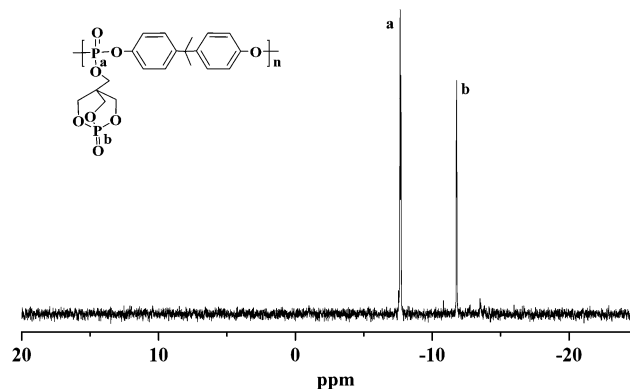


Fig. 3  $^{31}\text{P}$  NMR spectrum of PCPBO.

### 3.2 LOI and UL 94 test

To evaluate flammability of EP mixtures, Table 1 shows LOI and UL-94 results. As can be observed, pure EP is highly combustible, and its LOI value is 22.5%. The LOI value increases obviously with increase of PCPBO content. After incorporating 20 wt % PCPBO into the EP, the LOI value is significantly improved to 31.2% and UL-94 testing passes V-0 rating, whereas phosphorus-free EP shows no rating, indicating that PCPBO imparts excellent flame retardancy to epoxy resin.

### 3.3 Cone calorimetric analysis

Although LOI and UL94 testing are widely used in evaluating flame retardancy in polymer materials, they are not reliable indicators of likely performance in a real fire. For this kind of analysis, cone calorimeter is the most effective method and it can provide a wealth of parameters, including the time to ignition ( $t_{\text{ign}}$ ), the peak heat release rate (PHRR), the total heat release (THR) and average heat release rate (AHRR), of which the most important parameters are PHRR and THR.<sup>16</sup>

The flammability performance and the experimental data are presented in Fig. 4 and Table 2, respectively. It can be clearly seen from Fig. 4(a) that pure EP burns very fast after ignition and a sharp HRR peak appears with PHRR as high as  $1160.9 \text{ kW m}^{-2}$ . However, the addition of PCPBO leads to reduction in PHRR and the sample with 20 wt% PCPBO content exhibits the lowest PHRR value ( $337.1 \text{ kW m}^{-2}$ ), which is reduced by 71% compared to that of EP. It can be found that  $t_{\text{ign}}$  for EP/PCPBO systems is lower than that for EP (see Table 2) and much more lower with the increase of PCPBO incorporation because of the lower initial degradation temperature for PCPBO than that for EP. A similar phenomenon was observed by Song *et al.*<sup>17</sup> Moreover, the  $t_{\text{PHRR}}$  values for EP/PCPBO systems are postponed from 210 to 392 s with increasing content of PCPBO in EP. In the case of EP with 20 wt% PCPBO, its  $t_{\text{PHRR}}$  is 182 s longer than that of EP, indicating that PCPBO is an excellent flame retardant. It is worth noticing that there are two obvious peaks of the HRR curve of EP-PCPBO mixtures, which is a typical character of intumescent systems.<sup>18</sup> The first peak corresponds to the ignition and to the flame spread on the surface of the materials and then to protection *via* the

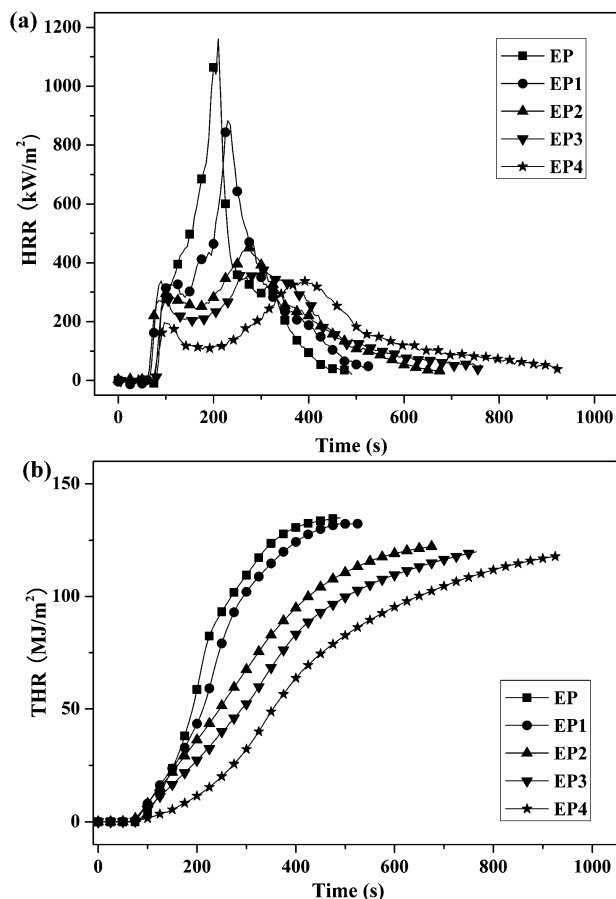


Fig. 4 HRR (a) and THR (b) curves of EP and EP-PCPBO mixtures.

Table 2 Cone calorimetry analysis data for EP mixtures at  $50 \text{ kW m}^{-2}$

Sample	$t_{\text{ign}}$ (s)	PHRR ( $\text{kW m}^{-2}$ )	AHRR ( $\text{kW m}^{-2}$ )	$t_{\text{PHRR}}$ (s)	THR ( $\text{MJ m}^{-2}$ )
EP	76	1160.9	328.8	210	135.0
EP1	65	882.8	306.6	230	132.1
EP2	61	460.5	198.6	270	122.3
EP3	44	375.4	177.4	305	119.8
EP4	31	337.1	142.9	392	117.3

<sup>a</sup> Residual char%: mass percentage left when testing finished.

intumescent coating when the HRR values become constant. The material is protected by the intumescent char in this time zone. The second peak means the destruction of the intumescent structure and the formation of a carbonaceous residue.

Fig. 4(b) presents THR curves for EP and its mixture. The slope of THR curve is assumed as representing the fire spread rate.<sup>19</sup> It can be found that the flame spread for EP-PCPBO mixtures decreases with the increase of PCPBO content in comparison with pure EP during the whole testing process, and the value of THR for EP4 is  $117.3 \text{ MJ m}^{-2}$ , which is reduced by 13.1% comparing with that of pure EP. Based on the results obtained from cone calorimetry, a conclusion can be drawn that

PCPBO is an effective flame retardant for EP because it could reduce significantly the HRR for EP during combustion.

Fig. 5 presents the digital photographs for the residues of EP and EP-PCPBO mixtures after LOI test (up) and cone calorimeter measurements (down). It is clearly seen from Fig. 5(a) and (a') that the residue of pure EP is not obviously expanded at the end of combustion. However, as for EP-PCPBO mixtures, the more the content of PCPBO, the more obvious the expansion is. As shown in Fig. 5(e') for EP/20 wt% PCPBO (EP4), it can be observed that the residual char after cone calorimeter test increases significantly. Moreover, the visual observation of the residues can be maintained and looks like a hill.

SEM is widely used as a tool to observe the morphology of the residual chars. Fig. 6 displays the SEM images of the surface residual chars for different samples after LOI test. As for pure EP, the surface of residual char appears uneven. Meanwhile, the

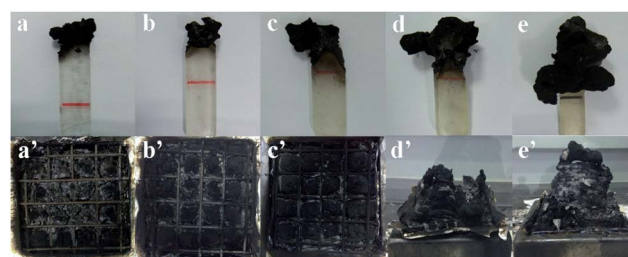


Fig. 5 Photographs of the char residues after LOI (a: EP; b: EP1; c: EP2; d: EP3; e: EP4) and cone calorimeter tests (a': EP; b': EP1; c': EP2; d': EP3; e': EP4).

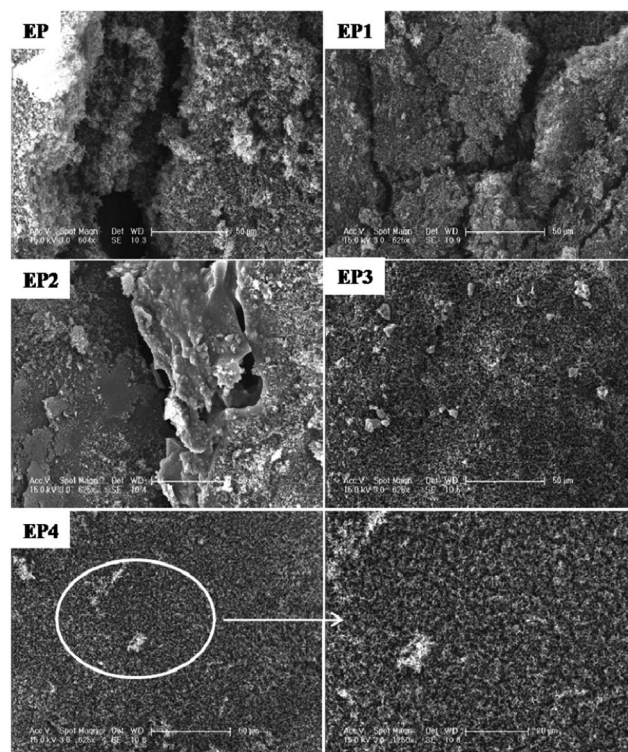


Fig. 6 SEM images of char residues for EP-PCPBO mixtures.

obvious cracks can be observed, and it is unable to swell and form an intumescent char layer. However, with the increase of PCPBO content, the surface of residual char becomes more and more compact and continuous. As can be seen from Fig. 6 (EP4), the surface of residue is tight, indicating the formation of a dense and cohesive char layer structure and against volatiles diffusion during the burning process. Thus, it can be found that the morphologies of residual char become compact with the increase of PCPBO content. This phenomenon coincides well with the results of the LOI and UL-94 test.

### 3.4 Thermal analysis

DSC is used to determine the glass transition temperature ( $T_g$ ), which is an important parameter for application of epoxy resin thermostets. The  $T_g$ s of EP and EP-PCPBO mixtures have been measured by DSC and the results are listed in Fig. 7 and Table 3. It can be found that the  $T_g$ s of flame retardant epoxy resins gradually decrease from 133 °C to 88 °C with increasing PCPBO content. The reason may be that the incorporation of PCPBO into the epoxy network will reduce its crosslink density and rigidity. This behavior is similar to the results of the ref. 20 and 21.

In order to investigate the effect of PCPBO on the thermal stability of epoxy resin, TGA was measured and analyzed. Fig. 8 illustrates TG and DTG curves of EP with different contents of PCPBO under air atmosphere, respectively. The temperature at

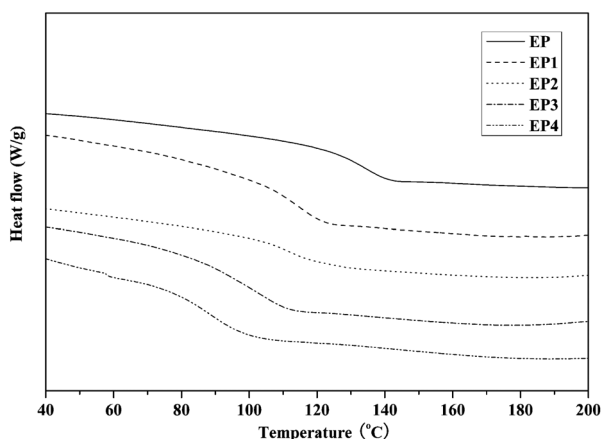


Fig. 7 DSC curves of EP and EP-PCPBO mixtures.

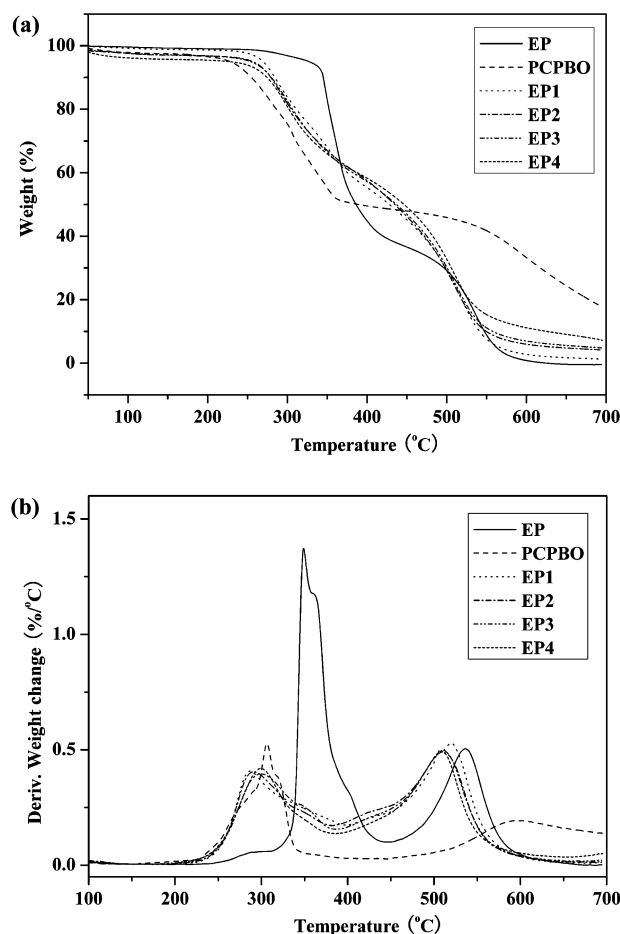


Fig. 8 TGA (a) and DTG (b) curves of EP and EP-PCPBO mixtures under air atmosphere.

which the weight loss is about 5% is determined as the initial decomposition temperature.  $T_{5\%}$ , the temperature at maximum rate of weight loss ( $T_{max}$ ), and the percentage of char yield at 700 °C are summarized in Table 3.

As can be observed in Fig. 8, the pure EP starts to decompose at 327 °C and the thermal oxidative degradation process mainly has two stages. The first stage is in the temperature range of 300–400 °C corresponding to a strong DTG peak at 349 °C. The second stage is in the temperature ranges of 400–550 °C corresponding to  $T_{max}$  of 536 °C. As for EP-PCPBO mixtures, the

Table 3 The thermal properties of EP and EP-PCPBO mixtures

Sample	$T_g$ (°C)	Air			Nitrogen		
		$T_{5\%}$ (°C)	$T_{max}$ (°C)	Char <sup>a</sup>	$T_{5\%}$ (°C)	$T_{max}$ (°C)	Char <sup>a</sup>
EP	133	327	349, 536	0.1	340	367	7.9
PCPBO	—	228	306, 591	17.7	234	354, 469	25.6
EP1	115	270	287, 520	1.3	304	355	11.7
EP2	110	256	292, 510	4.1	291	358	12.8
EP3	98	253	298, 510	4.8	284	360	15.9
EP4	88	227	299, 508	7.2	267	362	16.6

<sup>a</sup> Char yield at 700 °C.

thermal oxidative degradation process of all the samples have the similar two stages as the pure EP. However,  $T_{5\%}$  decreases when PCPBO content increases, which is probably due to the decomposition of P-C bonds which have lower thermal stability than C-C bonds.<sup>22</sup> In addition, the char yield for EP4 (with 20 wt%) increases to 7.2%.

From Fig. 9, the thermal degradation process under  $N_2$  atmosphere is different from that under air. The thermal degradation process of all samples has only one stage. When the PCPBO content increases,  $T_{5\%}$  decreases, showing a similar trend to the one mentioned above. It can be seen that the weight loss rate of the phosphorus-containing resin is significantly lower than that of the phosphorus-free resin under both air (Fig. 8(b)) and inert (Fig. 9(b)) atmosphere. This behavior is in accordance with the mechanism of improved flame retardancy *via* phosphorus modification:<sup>23</sup> the PCPBO can catalyze the polymer matrix to form an insulating protective layer, which reduces the weight loss rate, increases the thermal stability at higher temperatures, and improves the flame retardancy.

### 3.5 FT-IR study

In order to explore the details of the thermal oxidative behavior of EP and EP-PCPBO mixtures, the residues at different

temperatures were investigated by FTIR spectroscopy. Fig. 10 shows the FT-IR spectra of EP. The main characteristic peak of EP network can be observed at room temperature. The peak of O-H and N-H bonds ( $3200\text{--}3600\text{ cm}^{-1}$ ) nearly disappears at the temperature of  $250\text{ }^\circ\text{C}$ , which can be explained by the release of water and non-flammable gas molecule.<sup>24</sup> The relative intensity of the peak at  $1363\text{ cm}^{-1}$  for C-H bond in the  $C(CH_3)_2$  group decreases gradually with temperature increasing from 200 to  $330\text{ }^\circ\text{C}$  and disappears completely at above  $330\text{ }^\circ\text{C}$ , indicating that methyl side groups of EP are released. In addition, up to  $200\text{ }^\circ\text{C}$ , an evident decrease of peak of C-O-C at  $1035\text{ cm}^{-1}$  can be observed, which indicates that the scission of C-O occurring in the early step of thermal degradation of the epoxy network.<sup>25,26</sup> When the temperature rises up to  $350\text{ }^\circ\text{C}$ , it is found that the aliphatic components ( $2974\text{--}2867$  and  $1181\text{ cm}^{-1}$ ), aromatic ring C=C stretching vibration ( $1610$ ,  $1509$ , and  $1460\text{ cm}^{-1}$ ) and alkyl-aryl ether bonds ( $1240$  and  $1035\text{ cm}^{-1}$ ) decrease remarkably, suggesting that the main decomposition happens at this stage. This is consistent with the TGA results. It is worth noting that the aromatic ring C=C stretching vibration at  $1610$  and  $1509\text{ cm}^{-1}$  disappear, and a new broader peak at  $1595\text{ cm}^{-1}$  appears, indicating that the formation of polyaromatic carbons by crosslinking.<sup>27</sup> Furthermore, for the residue above  $350\text{ }^\circ\text{C}$ , their FTIR spectra are similar, indicating the chemical structure of residue became stable with consumption of this residue through the thermal oxidation process.

The FT-IR spectra of the EP4 at different degradation temperatures are shown in Fig. 11. It can be found that the relative intensities of  $CH_3$  stretching vibration at  $2964\text{--}2870\text{ cm}^{-1}$  and  $CH_3$  deformation vibration at  $1363\text{ cm}^{-1}$  decrease gradually from 200 to  $330\text{ }^\circ\text{C}$  and disappear completely at above  $350\text{ }^\circ\text{C}$ . Meanwhile, the peak at  $1036\text{ cm}^{-1}$  assigned to P-O-C bond disappears completely at  $300\text{ }^\circ\text{C}$ , indicating that P-O-C bond in PCPBO is not stable when heated. Moreover, the C=C stretching vibration of polyaromatic carbons at  $1594\text{ cm}^{-1}$  and some  $C_{Ar}\text{-H}$  deformation vibration at  $757\text{ cm}^{-1}$  could be detected at high temperature region, implying the formation of polyaromatic structures.<sup>24</sup> In addition, the new broad peak at

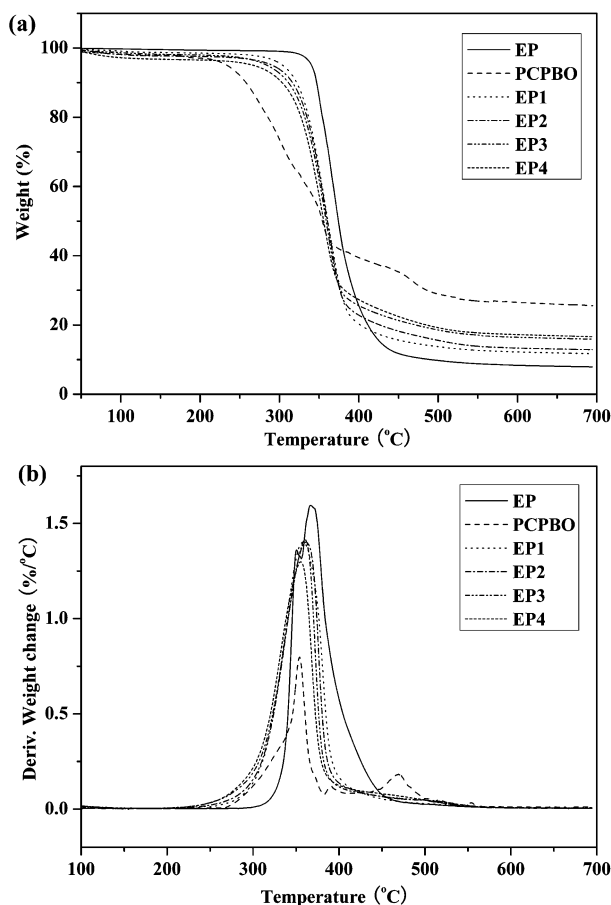


Fig. 9 TGA (a) and DTG (b) curves of EP and EP-PCPBO mixtures under nitrogen atmosphere.

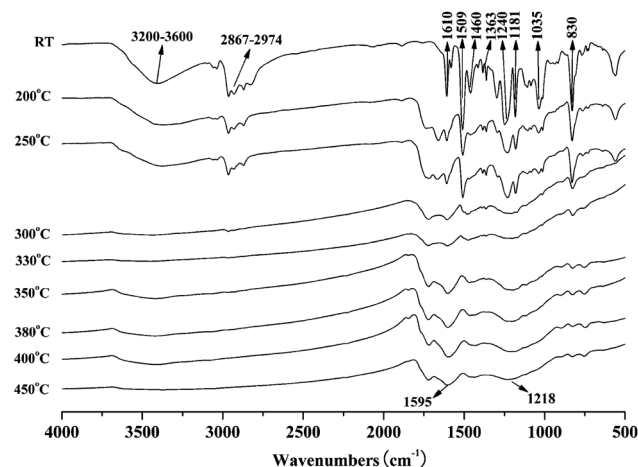


Fig. 10 FT-IR spectra of EP at different temperatures.

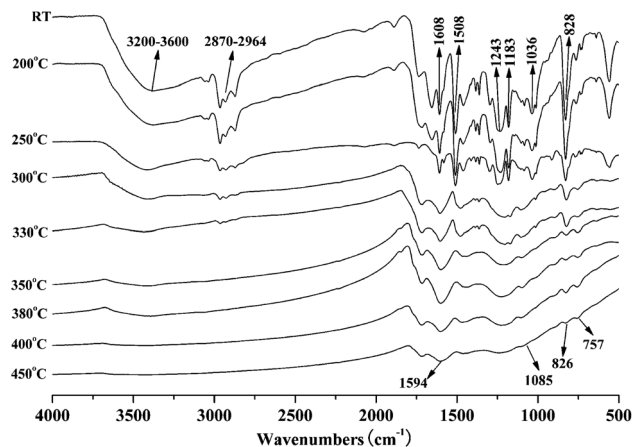


Fig. 11 FT-IR spectra of EP4 at different temperatures.

1085  $\text{cm}^{-1}$  appears, which means more C–O structure exist in the residue.<sup>28</sup>

Based on the experimental results and the relevant literature,<sup>12,29</sup> a possible route of the degradation process of PCPBO is illustrated in Fig. 12. It can be found that the two main decomposition products, including phosphate groups and some aromatic molecules, are produced in the degradation process. According to our previous research,<sup>30</sup> phosphate groups will further degrade into phosphoric acid and pentaerythriol. The phosphoric acid not only catalyzes the dehydration and charring of PER, but also produces a pyrophosphoric structure in the form of P–O–P in the condensed phase.<sup>12</sup> In addition, after isomerization and cyclization, pentaerythriol will form the stable char residue layer, which could prevent the heat transfer and protect the underlying materials from further burning and pyrolysis. Moreover, through a series of chemical reactions, including scission of main chain, crosslinking and thermal oxidation, the aromatic molecules eventually exist in form of polyaromatic carbons.

### 3.6 XPS study

The chemical components of the residual chars for EP and EP4 after cone calorimeter testing were investigated by XPS. As

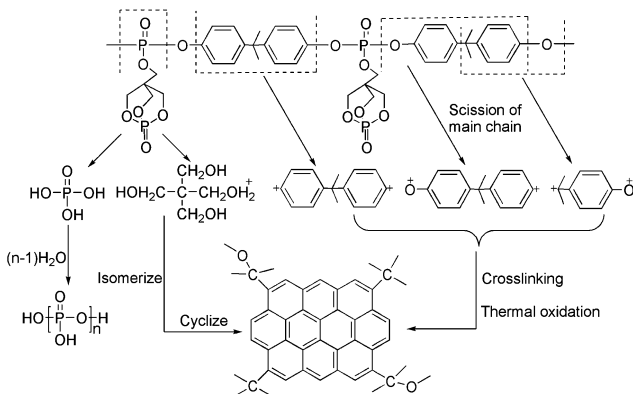


Fig. 12 Possible decomposition route of PCPBO.

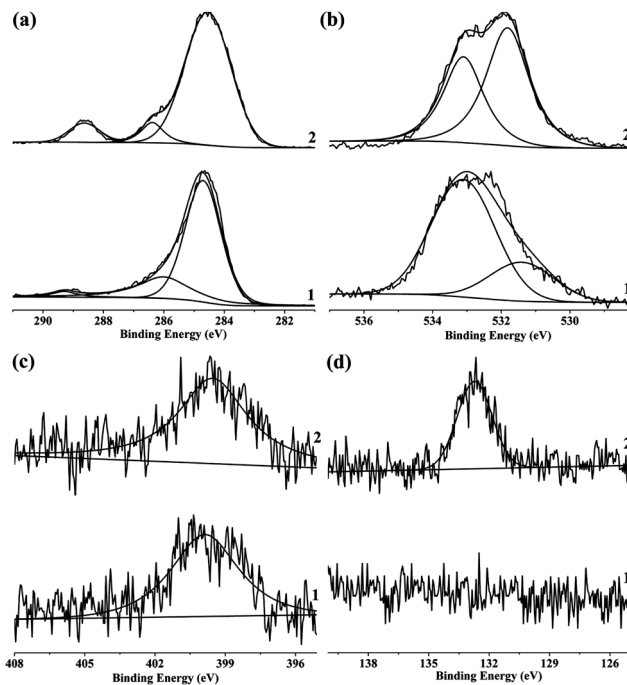


Fig. 13 (a)  $\text{C}_{1\text{s}}$ , (b)  $\text{O}_{1\text{s}}$ , (c)  $\text{N}_{1\text{s}}$  and (d)  $\text{P}_{2\text{p}}$  XPS spectra of residues of samples: 1-EP and 2-EP4.

Table 4 XPS results of the residual chars of EP and EP4

Sample	Binding energy (eV)	Atom (%)
<b>EP</b>		
$\text{C}_{1\text{s}}$	284.6, 286.0, 288.6	87.48
$\text{O}_{1\text{s}}$	531.8, 533.1	10.89
$\text{N}_{1\text{s}}$	400.1	1.61
$\text{P}_{2\text{p}}$	133.1	0.02
<b>EP4</b>		
$\text{C}_{1\text{s}}$	284.6, 286.0, 288.6	80.74
$\text{O}_{1\text{s}}$	531.8, 532.9	16.91
$\text{N}_{1\text{s}}$	400.1	1.49
$\text{P}_{2\text{p}}$	133.1	0.86

shown in Fig. 13(a) and Table 4, three bands are observed from  $\text{C}_{1\text{s}}$  spectra: the peak at 284.6 eV can be assigned to C–H and C–C in aliphatic and aromatic species, the peak at around 286.0 eV is assigned to C–O (ether and/or hydroxyl group), and another peak at around 288.6 eV corresponds to carbonyl groups.<sup>31</sup> Two bands at 531.8 eV and 533.1 eV are observed from  $\text{O}_{1\text{s}}$  spectra (Fig. 11(b)). It is reported that it is impossible to distinguish inorganic and organic oxygen because the  $\text{O}_{1\text{s}}$  band is structureless. The peak at 531.8 eV can be attributed to the =O in phosphate or carbonyl groups and the peak centered at 533.1 eV corresponds to –O– in C–O–C, C–O–P and/or C–OH groups. For the  $\text{N}_{1\text{s}}$  spectra, the peak at 400.1 eV corresponds to the formation of some oxidized nitrogen compounds. The single peak at 133.1 eV in  $\text{P}_{2\text{p}}$  spectrum can be assigned to the pyrophosphate and/or polyphosphate.<sup>32,33</sup> Furthermore, it can be seen from Table 4 that the atomic concentrations of

phosphorus and oxygen increase after addition of PCPBO, because of the crosslinking of phosphate and phosphate ester and the thermal oxidation of the aromatic molecules at high temperature, which leads to remaining the majority of phosphorus and oxygen in condensed phase. This phenomenon is coincided with the results of FTIR analysis.

## 4. Conclusions

A novel organophosphorus oligomer (PCPBO) was synthesized and characterized. A series of flame retardant epoxy resins with different PCPBO contents were prepared. The LOI values increased from 22.5% for the pure EP to 31.2% for phosphorus containing resins, and the EP materials with UL-94 V-0 were obtained with a PCPBO content of 20 wt%. The presence of PCPBO considerably reduced the flammability of EP, reflected by the reduction of PHRR and longer  $t_{\text{PHRR}}$ . For instance, compared to pure EP, the PHRR for EP containing 20 wt% PCPBO were reduced by 71%, with a  $t_{\text{PHRR}}$  of 182 s much longer than that of pure EP (210 s). The  $T_g$ s of flame retardant epoxy resins gradually decreased with increasing PCPBO content. TGA results indicated that the char yield and the thermal stability of the char increased with PCPBO content. The results from SEM observation showed that the formation of continuous and intact char residue effectively prevented the heat and oxygen approaching the EP matrix.

## Acknowledgements

This research is financially supported by the National Natural Science Foundation of China for the Projects (21204079, 50873099 and 51073149).

## Notes and references

- X. B. Huang, W. Wei, H. Wei, Y. H. Li, X. J. Gu and X. Z. Tang, *J. Appl. Polym. Sci.*, 2013, **130**, 248–255.
- P. P. Adroja, R. Y. Ghumara and P. H. Parsania, *Des. Monomers Polym.*, 2013, **16**, 503–508.
- S. Singh, V. K. Srivastava and R. Prakash, *Mater. Sci. Technol.*, 2013, **29**, 1130–1134.
- Q. Lv, J. Q. Huang, M. J. Chen, J. Zhao, Y. Tan, L. Chen and Y. Z. Wang, *Ind. Eng. Chem. Res.*, 2013, **52**, 9397–9404.
- M. Gao, W. H. Wu and Z. Q. Xu, *J. Appl. Polym. Sci.*, 2013, **127**, 1842–1847.
- M. Yin, L. Yang, X. Y. Li and H. B. Ma, *J. Appl. Polym. Sci.*, 2013, **130**, 2801–2808.
- F. Barontini, V. Cozzani, K. Marsanich, V. Raffa and L. Petarca, *J. Anal. Appl. Pyrolysis*, 2004, **72**, 41–53.
- S. Levchik, A. Piotrowski, E. Weil and Q. Yao, *Polym. Degrad. Stab.*, 2005, **88**, 57–62.
- W. C. Zhang, X. M. Li, H. B. Fan and R. J. Yang, *Polym. Degrad. Stab.*, 2012, **97**, 2241–2248.
- J. P. Ding, Z. Q. Tao, X. B. Zuo, L. Fan and S. Y. Yang, *Polym. Bull.*, 2009, **62**, 829–841.
- W. Z. Jiang, J. W. Hao and Z. D. Han, *Polym. Degrad. Stab.*, 2012, **97**, 632–637.
- J. Chen, S. M. Liu and J. Q. Zhao, *Polym. Degrad. Stab.*, 2011, **96**, 1508–1515.
- L. L. Zhang, A. H. Liu and X. R. Zeng, *J. Appl. Polym. Sci.*, 2009, **111**, 168–174.
- H. Q. Peng, Q. Zhou, D. Y. Wang, L. Chen and Y. Z. Wang, *J. Ind. Eng. Chem.*, 2008, **14**, 589–595.
- Y. Halpern, D. M. Mott and R. H. Niswander, *Ind. Eng. Chem. Prod. Res. Dev.*, 1984, **23**, 233–238.
- G. Gallina, E. Bravin, C. Badaluco, G. Audisio, M. Armanini, A. D. Chirico and F. Provasoli, *Fire Mater.*, 1998, **22**, 15–18.
- P. A. Song, Z. P. Fang, L. F. Tong and Z. B. Xu, *Polym. Eng. Sci.*, 2009, **49**, 1326–1331.
- J. Q. Huang, Y. Q. Zhang, Q. Yang, X. Liao and G. X. Li, *J. Appl. Polym. Sci.*, 2012, **123**, 1636–1644.
- A. B. Shehata, M. A. Hassan and N. A. Darwish, *J. Appl. Polym. Sci.*, 2004, **92**, 3119–3125.
- L. J. Qian, L. J. Ye, G. Z. Xu, J. Liu and J. Q. Guo, *Polym. Degrad. Stab.*, 2011, **96**, 1118–1124.
- L. P. Gao, D. Y. Wang, Y. Z. Wang, J. S. Wang and B. Yang, *Polym. Degrad. Stab.*, 2008, **93**, 1308–1315.
- U. Quittmann, L. Lecamp, W. El Khatib, B. Youssef and C. Bunel, *Macromol. Chem. Phys.*, 2001, **202**, 628–635.
- X. Wang, Y. Hu, L. Song and W. Y. Xing, *Polym. Bull.*, 2011, **67**, 859–873.
- X. Wang, Y. Hu, L. Song, H. Y. Yang, W. Y. Xing and H. D. Lu, *Prog. Org. Coat.*, 2011, **71**, 72–82.
- X. Wang, Y. Hu, L. Song, W. Y. Xing, H. D. Lu, P. Lv and G. X. Jie, *Polymer*, 2010, **51**, 2435–2445.
- W. C. Zhang, X. M. Li and R. J. Yang, *Polym. Degrad. Stab.*, 2010, **95**, 2541–2546.
- W. C. Zhang, X. M. Li, L. M. Li and R. J. Yang, *Polym. Degrad. Stab.*, 2012, **97**, 1041–1048.
- W. C. Zhang, X. M. Li and R. J. Yang, *J. Appl. Polym. Sci.*, 2013, **130**, 4119–4128.
- G. Camino, G. Martinasso, L. Costa and R. Gobetto, *Polym. Degrad. Stab.*, 1990, **28**, 17–38.
- N. N. Tian, X. Wen, J. Gong, L. Ma, J. Xue and T. Tang, *Polym. Adv. Technol.*, 2013, **24**, 653–659.
- L. Song, Q. L. He, Y. Yu, H. Chen and L. Liu, *Polym. Degrad. Stab.*, 2008, **93**, 627–639.
- K. Wu, Y. Hu, L. Song, H. D. Lu and Z. Z. Wang, *Ind. Eng. Chem. Res.*, 2009, **48**, 3150–3157.
- J. S. Wang, D. Y. Wang and Y. Liu, *J. Appl. Polym. Sci.*, 2008, **108**, 2644–2653.